

See discussions, stats, and author profiles for this publication at: <https://www.researchgate.net/publication/7520537>

Fabrication of Catalytic Membranes for the Treatment of Drinking Water Using Combined Ozonation and Ultrafiltration

ARTICLE *in* ENVIRONMENTAL SCIENCE AND TECHNOLOGY · NOVEMBER 2005

Impact Factor: 5.33 · DOI: 10.1021/es0503938 · Source: PubMed

CITATIONS

66

READS

24

4 AUTHORS, INCLUDING:



Melissa J Baumann

Auburn University

47 PUBLICATIONS 957 CITATIONS

SEE PROFILE



Susan J Masten

Michigan State University

79 PUBLICATIONS 1,708 CITATIONS

SEE PROFILE

Fabrication of Catalytic Membranes for the Treatment of Drinking Water Using Combined Ozonation and Ultrafiltration

BHAVANA S. KARNIK,[†]
SIMON H. DAVIES,[†]
MELISSA J. BAUMANN,[‡] AND
SUSAN J. MASTEN^{*†}

*Department of Civil and Environmental Engineering, and
Department of Chemical Engineering and Materials Science,
Michigan State University, East Lansing, Michigan 48824*

The removal of disinfection byproducts and their precursors was investigated using a combined ozonation–ultrafiltration system. A commercial membrane was coated 20 or 40 times with iron oxide nanoparticles (4–6 nm in diameter). With this membrane, the concentration of dissolved organic carbon was reduced by >85% and the concentrations of simulated distribution system total trihalomethanes and simulated distribution system halo acetic acids decreased by up to 90% and 85%, respectively. When the coated membrane was used, the concentrations of aldehydes, ketones, and ketoacids in the permeate were reduced by >50% as compared to that obtained with the uncoated membranes. Hydroxyl or other radicals produced at the iron oxide coated membrane surface as a result of ozone decomposition are believed to have enhanced the degradation of the natural organic matter, thereby reducing the concentration of disinfection byproducts. While increasing the number of times the membrane was coated from 20 to 40 did not significantly reduce the concentrations of most of the parameters measured, it did result in a significant decrease in the concentrations of ozonation byproducts. Increasing the sintering temperature from 500 to 900 °C also resulted in an improvement in the removal of the ozonation byproducts.

Introduction

The increased demand for drinking water has lead many water utilities to use source water containing elevated levels of natural organic matter (1, 2). This increasing demand, combined with stricter government regulations, necessitates improved drinking water treatment. The presence of natural organic matter (NOM) in the source water is a cause of concern to health professionals and environmental engineers because the reaction of NOM with disinfectants, such as chlorine, results in the formation of disinfection byproducts (DBPs), such as trihalomethanes (THMs) and haloacetic acids (HAAs). Because of their toxicity (3–5), the trihalomethanes and haloacetic acids are regulated by the U. S. Environmental Protection Agency (US EPA).

In the United States there is an increasing interest in the application of both ozone and membrane filtration for DBP

and DBP precursor removal in order to meet the requirements of the Surface Water Treatment Rule (SWTR), the Disinfectant and Disinfectant Byproducts Rule (D/DBPR), and the Long Term 1 Enhanced Surface Water Treatment rule (LT1ESWTR). Several researchers have attempted to combine ozone with polymeric membranes with limited success, in part because the organic membranes, which are commonly used in water and wastewater treatment applications, are prone to destruction by ozone (6–9). Hashino et al. (9) studied the use of ozonation combined with an ozone resistant polyvinylidene fluoride (PVDF) microfiltration membrane. They found that ozone prevented foulants from adhering to the membrane surface, thus decreasing membrane fouling. However, high dissolved ozone concentrations (>1 mg/L) were necessary to obtain high permeate fluxes and prevent membrane fouling.

Ceramic membranes are ozone resistant, and when these membranes are used in combination with ozone, stable permeate fluxes can be achieved without membrane damage (10–14). Kim and colleagues used ceramic membranes to investigate the effect of ozone bubbling on flux recovery (10). The results showed that intermittent ozonation effectively maintained high permeate fluxes and prevented membrane fouling caused by particle accumulation on the membrane surface (10). Our earlier work demonstrated that stable fluxes can be obtained with ozonation–ceramic membrane filtration. Ultrafiltration alone did not achieve the levels of treatment obtained with combined ozonation–membrane filtration. Ozonation–filtration resulted in a reduction of 50% in the dissolved organic carbon (DOC) concentration. It also resulted in the formation of partially oxidized compounds from NOM that were less reactive with chlorine, decreasing the concentration of simulated distribution system total trihalomethanes (SDS TTHMs) and simulated distribution system halo acetic acids (SDS HAAs) by up to 80% and 65%, respectively (12, 15).

Catalytic ozonation has been used to degrade NOM and other organic compounds in drinking water and wastewater (16). In the presence of different metal oxide catalysts, such as iron oxide, manganese oxide, titania, alumina, and zirconia, ozone degrades organic compounds, including saturated carboxylic acids, phenols, aromatic hydrocarbons, dyes, humic substances, and herbicides (17–23). On the basis of extensive research involving various ozonation methods for drinking water treatment, catalytic ozonation has been determined to be one of the best alternatives for the oxidation of ozone byproducts to carbon dioxide and the reduction in the chlorine demand (14, 24). Masten and Davies (25) reported that the presence of reactive soil surfaces catalyzed the decomposition of ozone and contaminants sorbed on the soil. Paillard et al. (26) documented that TiO₂-catalyzed ozonation was more efficient than ozone alone for the degradation of humic acid. Mn(II) is effective for the catalytic degradation of carboxylic acids that do not react appreciably with molecular ozone. It is believed that Mn(II) complexes with these carboxylic acids to form an intermediate byproduct that is more easily degraded by ozone (27–30). Ma and Graham (31, 32) confirmed that the degradation of compounds by ozone in the presence of manganese follows a radical mechanism. Pure alumina, which is often used as a support material for metal or metal oxide catalysts, was also found to be an effective catalyst for the degradation of NOM by ozone (33). Pecchi and Reyes (34) prepared iron oxide coatings supported on TiO₂ and Al₂O₃ using the sol–gel method. These coatings catalyzed the degradation of phenol by ozone.

* Corresponding author phone: (517)355-0228; fax: (517)355-0250; e-mail: masten@egr.msu.edu.

[†] Department of Civil and Environmental Engineering.

[‡] Department of Chemical Engineering and Materials Science.

This work focuses on the fabrication of ceramic membranes with catalytic properties using a layer-by-layer method to deposit iron oxide particles on a titania-coated membrane. We have tested the application of these membranes in a combined ozonation-ultrafiltration process to remove disinfection byproducts and their precursors.

Experimental Section

Membrane Preparation and Characterization. Tubular AZT (a mixture of alumina, zirconia, and titania) ceramic membranes (clover-leaf design (containing three channels), CéRAM Inside, TAMI North America, St. Laurent, Québec, Canada) with nominal molecular weight cutoffs of 15 kilodaltons (kDa) and 5 kDa were used as a support for the catalytic coatings. The external diameter of each membrane was 10 mm, and the active membrane length was 8 cm. The total filtering area of the membrane was approximately 11 cm², and the membranes can be operated in the pH range from 0 to 14. The initial permeability of the membranes was tested using DDI water (12).

The colloidal particles used for coating the membranes were prepared by Sorum's method as described by Mulvaney et al. (35). The procedure used was as follows: double-deionized water (DDI) water (450 mL) was heated until it boiled vigorously; then 50 mL of freshly prepared 20 mM FeCl₃ solution was added at a rate of approximately two drops per second. The sol rapidly turned golden brown and finally deep red. After all the ferric chloride solution was added, the suspension was allowed to boil for an additional 5 min; it was then cooled to room temperature and dialyzed, using cellulose dialysis tubing with an average flat width of 33 mm for 48 h against a dilute nitric acid solution having a pH of 3.5.

Transmission electron microscopy (TEM) characterization was performed using a JEOL 100CX at an accelerating potential of 100 kV with magnifications ranging from 5000× to 370 000×. The TEM protocol for the particle characterization involved diluting the suspension with DDI water in the ratio of 1:4. Double-sided sticky tape was attached to a glass slide (76.2 mm × 25.4 mm × 1 mm), leaving a small section (approximately 2–3 mm) of the tape hanging off the long side of the slide. Masking tape was then used to cover the portion of the double-sided tape, which rested on the glass slide, leaving the excess double-sided sticky tape uncovered. Grids (0.25% Formvar and carbon) were placed on the overhanging double-sided sticky tapes with light tweezer pressure to ensure that the grids would stick. The suspension was then placed in a dropwise manner onto the grids, and the excess suspension was removed by lightly wiping across the grid with filter paper. The grids were then air-dried in a dust free environment until TEM analysis. Photomicrographs were collected using a Megaview III digital camera. The photomicrographs, which are provided in the Supporting Information, showed that the average particle diameter was 4–6 nm.

The layer-by-layer technique used to coat the membranes is based on a protocol described by McKenzie et al. (36) for coating doped tin oxide electrodes. The membrane was immersed in the colloidal suspension for 1 min and then rinsed with DDI water. Then, the membrane was immersed in an aqueous phytic acid (40 mM) for 1 min and rinsed with the DDI water. This sequence was repeated the desired number of times (20 or 40). After coating, the membrane was either sintered at 500 °C for 60 min or sintered at 900 °C for 30 min. These two temperatures were chosen to produce membranes on which the iron oxide particles were attached but not fused to each other (500 °C) or completely sintered to each other and to the membrane surface (900 °C).

Ozonation/Membrane Filtration. A schematic representation of the ozonation–membrane system (12, 15) is shown

TABLE 1. Operating Conditions for the Ozone–Membrane Filtration System

| | |
|------------------------------|----------------------|
| water recirculation rate | 2.75 L/min |
| water temperature | 20 °C |
| ozone gas flow rate | 100 mL/min |
| transmembrane pressure (TMP) | 0.5 bar |
| gaseous ozone concentration | 2.5 g/m ³ |

in the Supporting Information. A stainless steel filter holder, Teflon tubing, and stainless steel or Teflon joints and valves were used throughout the system. Other components included 3.5 L and 1.5 L water-jacked glass reservoirs made of Pyrex glass and a simple Y inline mixer (Ozone Service, Burton, BC, Canada). The membranes described above were used for membrane filtration. A Teflon valve was placed in the retentate line of the membrane system to create transmembrane pressures of 0.2–0.5 bar. Ozone gas was added into the water stream through a simple Y inline mixer, just before the aqueous stream entered the membrane module.

To generate ozone, pure oxygen gas (99.999%) from a pressurized cylinder was dried using a molecular sieve trap and then fed to the ozone generator (model OZ2PCS, Ozotech Inc., Yreka, CA). The voltage applied to the ozone generator was varied to control the gaseous ozone concentration. The excess gas was vented to the atmosphere after it was passed through a 2% potassium iodide (KI) solution to destroy any residual ozone. The water in the 3.5 L reservoir was maintained at a constant level during the experiments using a peristaltic pump (Masterflex model 7520-35, Cole-Parmer Co., Chicago, IL) to transfer the water from a 1.5 L reservoir into the 3.5 L reservoir. A constant water temperature of 20 °C was maintained using a recirculating water bath. The experiments were performed with a membrane cross-flow velocity of 0.6 m/s; the flow was turbulent with a Reynolds number of approximately 6000.

The operating conditions are shown in Table 1. The operating conditions were determined based on the previous experiments with uncoated membranes (12, 15, 41). The conductivity remained practically unchanged for the duration of the experiment. The change in conductivity was <0.01 μS/cm.

Permeate samples were collected in bottles covered with Parafilm and stored in an ice-bath throughout the duration of the experiment. The first 400 mL of permeate collected was labeled as P1 and the latter 1000 mL as P2.

Water Source. Experiments were carried out using samples taken from Lake Lansing (Haslett, MI), which is a borderline eutrophic lake. The typical characteristics of the water from Lake Lansing (37) are given in Table S1 in the Supporting Information. The samples were collected at the boat ramp at the Lake Lansing Park-South, Haslett, MI in 5 gal polyethylene carboys and stored at 4 °C. The maximum storage period was 7 days. Water samples were prefiltered through a 0.45 μm mixed cellulose ester filter (Millipore-HA) before testing.

Analytical Methods. The absorbance of ozone in the gas phase was measured at 254 nm with a Milton Roy Genesis-5 spectrophotometer (Milton Roy, Inc., Rochester, NY) using a 2 mm path length quartz flow-through cell. An extinction coefficient of 3000 M⁻¹ cm⁻¹ (38) was used to calculate the ozone concentration.

The ultraviolet (UV) absorbance of the water samples was measured at a wavelength of 254 nm with a Milton Roy Genesis-5 spectrophotometer (Milton Roy, Inc., Rochester, NY) using a 1 cm quartz cell.

DOC was analyzed using an OI Analytical model 1010 analyzer using the UV/persulfate method (39). To ensure method reliability, standards having TOC concentrations of 2.5, 5, 7, and 10 mg/L (OI Analytical) were run with every set

of samples. Samples were analyzed in triplicate. A blank was also run with every set of samples.

The concentrations of humic substances in the samples were measured by adsorption on an XAD-8 resin according to Standard Method 5510C (39). A 100 mL sample was acidified with concentrated phosphoric acid to a pH of 2; the acidified sample was then eluted through a 10 mm diameter (i.d.) \times 15 cm long column at a flow rate of 2 mL/min. The effluent from the column was collected and then analyzed for TOC, which represents the nonhumic fraction of the dissolved organic matter in the water sample. The resin-packed column was then back eluted with 100 mL of 0.1 N sodium hydroxide at a flow rate of 2 mL/min. The eluent was collected and acidified with concentrated phosphoric acid to a pH less than 4, purged with high-purity helium for 3 min to remove the inorganic carbon, and analyzed for TOC. The organic content of the eluent represents the concentration of humic substances.

Water samples were dosed with a chlorine concentration that ensured a residual chlorine concentration in the range of 0.5–mg/L after 48 h of incubation at room temperature, according to the procedures in Standard Method 2350 (39). The THM compounds, chloroform (CHCl_3), bromodichloromethane (CHBrCl_2), dibromochloromethane (CHBr_2Cl), and bromoform (CHBr_3), were extracted from the water samples using hexane and analyzed by gas chromatography Standard Method 5710 (39). A Perkin-Elmer Autosystem gas chromatograph (Perkin-Elmer Instruments, Shelton, CT) equipped with an electron capture detector (ECD), an autosampler, and a 30 m \times 0.25 mm i.d., 1 μm DB-5ms column (J&W Scientific, Folsom, CA) was used for the analysis. The oven temperature was ramped from 50–150 $^\circ\text{C}$ at a rate of 10 $^\circ\text{C}/\text{min}$. The flow rate of the carrier gas (N_2) was 10 mL/min. The injector temperature and detector temperature were 275 and 350 $^\circ\text{C}$, respectively.

SDS HAAs were produced by chlorination as described above. The concentrations of monochloroacetic acid (MCAA), monobromoacetic acid (MBAA), dichloroacetic acid (DCAA), bromochloroacetic acid (BCAA), trichloroacetic acid (TCAA), and dibromoacetic acid (DBAA) were determined using US EPA Method 552.2. A Perkin-Elmer Autosystem gas chromatograph (Perkin-Elmer Instruments, Shelton, CT) equipped with an ECD, an autosampler, and a 30 m \times 0.32 mm i.d., 3 μm DB-1 column (J&W Scientific, Folsom, CA) was used for the analysis. The oven temperature was programmed to hold for 15 min at 32 $^\circ\text{C}$, then increased to 75 $^\circ\text{C}$ at a rate of 5 $^\circ\text{C}/\text{min}$ and held 5 min, then increased to 100 $^\circ\text{C}$ at a rate of 5 $^\circ\text{C}/\text{min}$. The carrier flow (N_2) was 10 mL/min with the injector and detector temperatures at 200 and 260 $^\circ\text{C}$, respectively.

US EPA Method 556 (40) was used to monitor formaldehyde, propionaldehyde, glyoxal, methyl glyoxal, acetone, and 2-butanone, ketomalonic acid, pyruvic acid, and glyoxylic acid. A Perkin-Elmer Autosystem gas chromatograph (Perkin-Elmer Instruments, Shelton, CT) equipped with an ECD, an autosampler, and a 30 m \times 0.25 mm i.d., 0.5 μm DB-5ms column (J&W Scientific, Folsom, CA) was used in the analysis. The oven temperature was programmed to hold at 1 min at 50 $^\circ\text{C}$, then increased to 220 $^\circ\text{C}$ at a rate of 4 $^\circ\text{C}/\text{min}$ followed by an increase to 250 $^\circ\text{C}$ at a rate of 20 $^\circ\text{C}/\text{min}$ with a 5 min hold time. The carrier flow was 1.0 mL/min, and the injector and detector temperatures were 180 and 300 $^\circ\text{C}$, respectively.

Results and Discussion

Our earlier work showed no significant decrease in the permeate flux when using ozone at gas-phase concentrations greater than 2.5 g/m³ (12). Experiments were conducted to determine the effect of the coating procedure on membrane permeability. As shown in Figure 1, stable fluxes were maintained throughout the course of each experiment. The

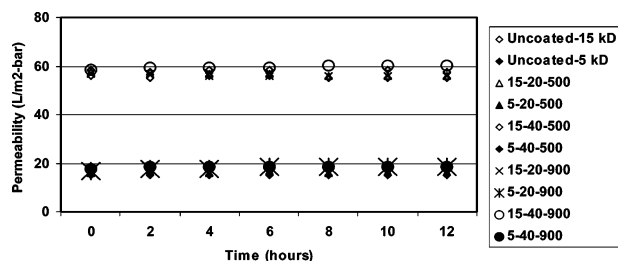


FIGURE 1. Permeate flux for different membrane-coating modifications. Experimental setup: Figure S1 in the Supporting Information. Operating conditions: Table 1. Membrane size: 5 or 15 kDa. All values are the average of triplicates within experiments and duplicate experiments. The values have a maximum standard deviation of 5%. For the coated membranes the first number in the legend corresponds to the MWCO of the membrane, the second number is the number of coatings, and the third number is the sintering temperature. For example, 15–20–500 is a membrane with 15 kDa MWCO coated 20 times with the catalyst and sintered at 500 $^\circ\text{C}$. All values are the average of triplicates within experiments.

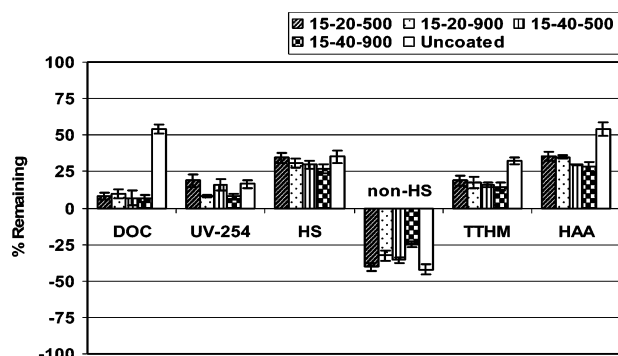


FIGURE 2. Water quality results for two different sintering temperatures. Experimental setup: Figure S1 in the Supporting Information. Operating conditions: Table 1. Membrane size: 15 kDa. Coating: 20 or 40 coatings. Sintering temperature: 500 or 900 $^\circ\text{C}$. All values are average of triplicates within experiments. Explanation of the legend is given in the caption of Figure 1.

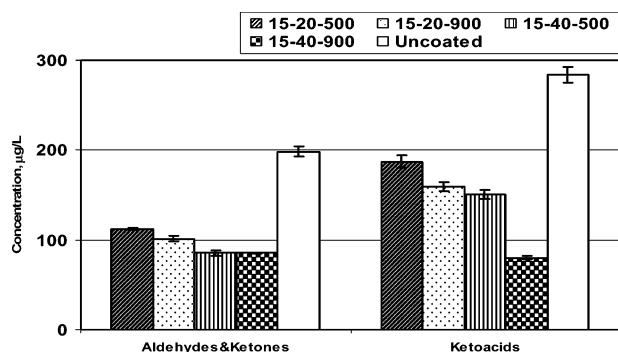


FIGURE 3. Concentrations of ozonation byproducts in the permeate for two different sintering temperatures. Experimental setup: Figure S1 in the Supporting Information. Operating conditions: Table 1. Membrane size: 15 kDa. Coating: 20 or 40 coatings. Sintering temperature: 500 or 900 $^\circ\text{C}$. All values are the average of triplicates within experiments. Explanation of the legend is given in the caption of Figure 1.

coating of the membrane had little effect on its permeability, suggesting that processing did not damage the integrity of the membrane and that the resistance of the iron oxide coating is comparatively small.

Figures 2–5 compare the results obtained for the coated and uncoated membranes. The results for the 15 kDa membrane are shown in Figures 2 and 3, and Figures 4 and 5 show the results for the 5 kDa membrane. As shown in

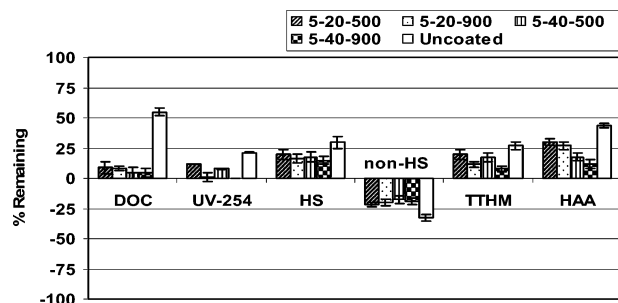


FIGURE 4. Water quality results for two different sintering temperatures. Experimental setup: Figure S1 in the Supporting Information. Operating conditions: Table 1. Membrane size: 5 kDa. Coating: 20 or 40 coatings. Sintering temperature: 500 or 900 °C. All values are the average of triplicates within experiments. Explanation of the legend is described in the caption of Figure 1.

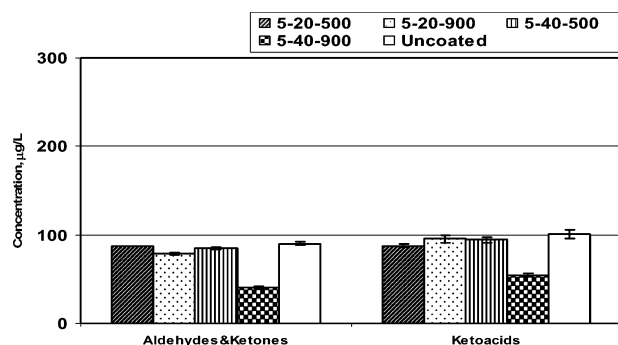


FIGURE 5. Concentrations of ozonation byproducts in the permeate for two different sintering temperatures. Experimental setup: Figure S1 in the Supporting Information. Operating conditions: Table 1. Membrane size: 5 kDa. Coating: 20 or 40 coatings. Sintering temperature: 500 or 900 °C. All values are the average of triplicates within experiments. Explanation of the legend is described in the caption of Figure 1.

Figure 2, the permeate fluxes are different for the 15 and 5 kDa MWCO membranes. Thus, due to the different ozone contact times, a direct comparison of the results for the membranes with different MWCOs is impossible.

Figures 2 and 4 show that the reduction in the DOC concentration in the P2 samples is greater for the coated membranes than for the uncoated membrane. This reduction in DOC concentrations suggests that the iron oxide coating catalyzes the degradation of ozone to produce radical species at the membrane surface, which degrade the NOM. Losses due to sorption of NOM on the iron oxide coating are expected to be very small, since the iron oxide coatings are extremely thin. On the basis of the observed thickness of the coating (using TEM), the total quantity of iron oxide deposited on the membrane is estimated to be less than 0.1 µg. The quantity of DOC removed is estimated to be >4 mg C. To remove this amount of NOM via sorption, the sorptive capacity of the iron oxide would have to be of the order of 4×10^7 g/kg. This figure is too large to be reasonable, even for nanoparticles, so we conclude that sorption to the iron oxide particles cannot explain the enhanced NOM removal seen with the coated membranes. As with all parameters measured, the results for NOM removal in the P1 samples follow the same trends as observed with P2 samples. As such, only the data for P2 samples is presented in the figures. The data for P1 samples is available in the Supporting Information.

There is a little difference between the coated and uncoated membranes in the extent to which the absorbance of the UV-254 absorbing compounds is reduced. In our earlier work, we showed that the removal of the UV-254 absorbing compounds is predominately due to the reaction of ozone

with these substances and not due to filtration (15). Together, these results suggest that the reduction in UV-absorbing compounds is due to solution phase ozonation rather than surface catalytic reactions.

Similarly, no statistically significant differences were observed in the concentrations of the humic substances found in the permeate after combined treatment of ozonation–membrane filtration using either the coated and uncoated membranes. Consistent with these results for the removal of humic substances, the concentrations of non-humic substances formed were also similar in the permeates from all membranes studied (see Figures 2 and 4). The behavior of HS and non-HS in the ozone–membrane filtration system is discussed in detail in our earlier work, where we studied the destruction of HS and formation of the non-HS during ozonation alone, membrane filtration alone, and in the hybrid process (15). The concentration of HS remaining in the P2 samples after ozonation–membrane filtration was less than 50% of that in the raw water. This reduction is, in part, due to the reaction of NOM with either ozone or OH radicals, since an increase in the nonhumic substance (non-HS) concentration after ozonation–filtration was observed. The increase in non-HS concentration could only be caused by the conversion of HS to non-HS. Filtration would not have resulted in such a conversion. This conclusion is substantiated by results presented by Karnik et al. (15), which show that the percent removal of HS using ultrafiltration was 13% for P2, while 50% of the HS was removed by ozonation.

The concentrations of non-HS measured in the P2 samples increased by approximately 20% compared to that in the P1 samples, indicating that the reaction of HS to form non-HS continued throughout the course of the experiment. If the humic substances were removed purely by filtration, the extent of removal would not likely have increased with ozonation time.

Despite the results for HS, the extent to which the DBPs precursors were removed was greater with the coated membranes than with the uncoated membrane (see Figures 2 and 4). The concentrations of TTHMs and HAAs were reduced by up to 90% and up to 85%, respectively, with ozonation combined with an iron oxide coated 5 kDa membrane. The membrane surface coated with iron oxide appears to catalyze reactions that lead to a reduction in DBPs and DBP precursors. For the 15 kDa membranes, the concentrations of aldehydes, ketones, and ketoacids in the permeate following treatment using the coated membranes were less than that obtained with the uncoated membrane (see Figure 3). Ozone may decompose on the active metal sites of the iron oxide surface, resulting in increased rates of hydroxyl radical production (31–33), which in turn leads to a concomitant decrease in the concentration of disinfection byproducts and their precursors.

To improve the adhesion of the coating to the membrane, several coated membranes were sintered at 900 °C. The results for the coated membranes treated at 500 and 900 °C are compared in Figures 2 to 5. A small decrease in the concentration of ozonation byproducts was found when the higher sintering temperature was used. It appears that sintering at higher temperatures alters the properties of the ceramic membrane surface, which further enhances its catalytic properties. Ongoing studies are being conducted using scanning electron microscopy (SEM) and TEM imaging of these sintered surfaces along with chemical and phase analysis of the membrane surface to better understand the changes that occur during sintering.

As seen in Figures 2–5, increasing the number of coatings of iron oxide did not result in a significant improvement in the system performance, except for the ozonation byproducts. The lowest concentrations of aldehydes, ketones, and ke-

toacids were achieved using the membrane that was coated 40 times and sintered at 900 °C. The 5 kDa membrane performed better than the 15 kDa membrane. A statistical analysis of the data presented in Figures 2-5 using ANOVA indicates that at the 95% confidence level, with the exception of the results for HAAs with a 5 kDa membrane (see Figure 4) and the ozonation byproducts with a 15 kDa membrane (see Figure 3), there is no statistically significant difference for the removal of NOM, DBPs, or DBP precursors using the membranes coated 20 or 40 times.

The US EPA, under the Stage 2 Disinfection/Disinfection By-Product (D/DBP) Rule, sets standards for maximum DBP concentrations in drinking water. The maximum contaminant levels for TTHMs and HAAs are 80 µg/L and 60 µg/L, respectively. Catalytic ozonation membrane filtration met regulatory limits for both contaminants. With the use of a 5 kDa MWCO membrane, coated 20 times and sintered at 900 °C, the concentrations of TTHMs and HAAs after chlorination were approximately 25–30 µg/L and 20–25 µg/L, respectively. Even better quality water was achieved using a 5 kDa MWCO membrane, coated 40 times and sintered at 900 °C. After chlorination the concentration of TTHMs was approximately 15–20 µg/L and the concentration of HAAs was approximately 7–15 µg/L. These results are especially significant because these limits are difficult to meet with poor quality waters, such as those used in this work.

Previous work has demonstrated we can meet the regulatory requirements for DBPs using a 1 kDa membrane and a gaseous ozone concentration of 2.5 g/m³ (15). Comparable results could be obtained using iron oxide coated 5 kDa membranes. As the permeability of the 5 kDa membrane is 3 times greater than that of the 1 kDa membrane, a significant decrease in the costs associated with the process can be achieved using the coated membrane while still producing high quality water that meets the pertinent regulatory requirements of the Stage 2 D/DBP Rule.

Acknowledgments

The authors acknowledge the U.S. Environmental Protection Agency (US EPA) Science To Achieve Results (STAR) Program (Grant No. RD830090801) for financial support of this work. We also thank Nikhil Theyyuni for his assistance with the membrane-coating process. Dr. Alicia Pastor from the Center for Advanced Microscopy is also acknowledged for her assistance with the TEM sample preparation.

Supporting Information Available

Data showing water quality for permeate 1 (P1) of the 15 and 5 kDa MWCO is available in Figures S1–S7. The effect of sintering temperatures on the permeates of 15 and 5 kDa MWCO is shown in Figures S8 and S9. Figure S10 is the TEM image of iron oxide particles used in coating the membranes, and S11 is the TEM image of coated ceramic membrane. This material is available free of charge via the Internet at <http://pubs.acs.org>.

Literature Cited

- Bursill, D. Drinking water treatment—understanding the processes and meeting the challenges. *Water Sci. Technol. Water Supply* **2001**, *1*, 1–7.
- Skjelkvåle, B. L.; Andersen, T.; Halvorsen, G. A.; Raddum, G. G.; Heegaard, E.; Stoddard, J.; Wright, R. The 12-year report: Acidification of surface waters in Europe and North America; trends biological recovery and heavy metals. *ICP—Waters Report* **2000**, *52*, 115.
- Morris, R. D.; Audet, A. M.; Angelillo, I. F.; Chalmers, T. C.; Mosteller, F. Chlorination, chlorination byproducts, and cancer—a metaanalysis. *Am. J. Public Health* **1992**, *82*, 955–963.
- Mughal, F. H. Chlorination of drinking water and cancer: A review. *Pathol. Toxicol. Oncol.* **1992**, *11*, 287–292.
- Kool, H. J.; van Kreijl, C. F.; Hrubec, J. Mutagenic and carcinogenic properties of drinking water. In: *Water Chlorination: Chemistry, Environmental Impacts, and Health Effects*; Jolley, R. L., Brungs, W. A., Cumming, R. B., Eds.; Lewis Publishers: Chelsea, MI, 1985.
- Shanbhag, P. V.; Guha, A. K.; Sirkar, K. K. Membrane-based ozonation of organic compounds. *Ind. Eng. Chem. Res.* **1998**, *37*, 4388–4398.
- Castro, K.; Zander, A. K. Membrane air-stripping—effects of pretreatment. *J. Am. Water Works Assoc.* **1995**, *87*, 50–61.
- Shen, Z. S.; Semmens, M. J.; Collins, A. G. A novel approach to ozone water mass-transfer using hollow fiber reactors. *Environ. Technol.* **1990**, *11*, 597–608.
- Hashino, M.; Mori, Y.; Fujii, Y.; Motoyama, N.; Kadokawa, N.; Hoshikawa, H.; Nishijima, W.; Okada, M. Pilot plant evaluation of an ozone-microfiltration system for drinking water treatment. *Water Sci. Technol.* **2000**, *41*, 17–23.
- Kim, J. O.; Somiya, I. Effective combination of microfiltration and intermittent ozonation for high permeation flux and VFAs recovery from coagulated raw sludge. *Environ. Technol.* **2001**, *22*, 7–15.
- Kim, J. O.; Somiya, I.; Fujii, S. Fouling control of ceramic membrane in an organic acid fermenter by intermittent ozonation. Proceedings of the 14th Ozone World Congress, Dearborn, MI, 1999; International Ozone Association: Stamford, CT, 1999; pp 131–143.
- Karnik, B. S.; Davies, S. H.; Chen, K. C.; Jaglowski, D. R.; Baumann, M. J.; Masten, S. J. Effects of ozonation and pH on the permeate flux of nanocrystalline ceramic membranes. *Water Res.* **2005**, *39*, 728–734.
- Schlichter, B.; Mavrov, V.; Chmiel, H. Study of a hybrid process combining ozonation and microfiltration/ultrafiltration for drinking water production from surface water. *Desalination* **2004**, *168*, 307–317.
- Allemane, H.; Deloune, B.; Paillard, H.; Legube, B. Comparative efficiency of three systems (O₃/O₃H₂O₂ and O₃/TiO₂) for the oxidation of natural organic matter in water. *Ozone Sci. Eng.* **1993**, *15*, 419–432.
- Karnik, B. S.; Davies, S. H.; Baumann, M. J.; Masten, S. J. The effects of combined ozonation and filtration on disinfection byproduct formation. *Water Res.* **2005**, *39*, 2839–2850.
- Legube, B.; Karpel Vel Leitner, N. Catalytic ozonation: A promising advanced oxidation technology for water treatment. *Catal. Today* **1999**, *53*, 61–72.
- Beltran, F. J.; Rivas, F. J.; Montero-de-Espinosa, R. Ozone enhanced oxidation of oxalic acid in water with cobalt catalysts. 1. Homogeneous catalytic ozonation. *Ind. Eng. Chem. Res.* **2003**, *42*, 3210–3217.
- Beltran, F. J.; Rivas, F. J.; Montero-de-Espinosa, R. Ozone enhanced oxidation of oxalic acid in water with cobalt catalysts. 2. Heterogeneous catalytic ozonation. *Ind. Eng. Chem. Res.* **2003**, *42*, 3218–3224.
- Radhakrishnan, R.; Oyama, S. T. Ozone decomposition over manganese oxide supported on ZrO₂ and TiO₂: A kinetic study using in situ laser Raman spectroscopy. *J. Catal.* **2001**, *199*, 282–290.
- Ni, C. H.; Chen, J. N. Heterogeneous catalytic ozonation of 2-chlorophenol aqueous solution with alumina as a catalyst. *Water Sci. Technol.* **2001**, *43*, 213–220.
- Gracia, R.; Cortes, S.; Sarasa, J.; Ormad, P.; Ovelheiro, J. L. Catalytic ozonation with supported titanium dioxide: The stability of catalyst in water. *Ozone Sci. Eng.* **2000**, *22*, 185–193.
- Gracia, R.; Cortes, S.; Sarasa, J.; Ormad, P.; Ovelheiro, J. L. Heterogeneous catalytic ozonation with supported titanium dioxide in model and natural waters. *Ozone Sci. Eng.* **2000**, *22*, 461–471.
- Gracia, R.; Aragües, J. L.; Ovelheiro, J. L. Study of the catalytic ozonation of humic substances in water and their ozonation byproducts. *Ozone Sci. Eng.* **1996**, *18*, 195–208.
- Volk, C.; Roche, P.; Joret, J. C.; Paillard, H. Comparison of the effect of ozone, ozone-hydrogen peroxide system and catalytic ozone on the biodegradable organic matter of a fulvic acid solution. *Water Res.* **1997**, *31*, 650–656.
- Masten, S. J.; Davies, S. H. R. Efficacy of in-situ ozonation for the remediation of PAH contaminated soils. *J. Contam. Hydrol.* **1997**, *28*, 327–335.
- Paillard, H.; Dore, M.; Bourbigout, M. M. Prospects concerning applications of catalytic ozonation in drinking water treatment. Proceedings of the 10th Ozone World Congress, Monaco, March 1991; International Ozone Association: Zurich, Switzerland, 1991; pp 313–329.

- (27) Andreozzi, R.; Marotta, R.; Sanchirico, R. Manganese catalyzed ozonation of glyoxalic acid in aqueous solutions. *J. Chem. Technol. Biotechnol.* **2000**, 75, 59–65.
- (28) Andreozzi, R.; Caprio, V.; Insola, A.; Marotta, R.; Tufano, V. The ozonation of pyruvic acid in aqueous solutions catalyzed by suspended and dissolved manganese. *Water Res.* **1998**, 32, 1492–1496.
- (29) Andreozzi, R.; Caprio, V.; Insola, A.; Marotta, R.; Tufano, V. The use of manganese dioxide as a heterogeneous catalyst for oxalic acid ozonation in aqueous solutions. *Appl. Catal., A.* **1998**, 131, 75–81.
- (30) Andreozzi, R.; Insola, A.; Caprio, V.; D'Amore, M. G. The kinetics of Mn(II) catalyzed ozonation of oxalic acid in aqueous solutions. *Water Res.* **1992**, 26, 917–921.
- (31) Ma, J.; Graham, N. J. D. Degradation of atrazine by manganese-catalyzed ozonation-influence of radical scavengers. *Water Res.* **2000**, 34, 3822–3828.
- (32) Ma, J.; Graham, N. J. D. Degradation of atrazine by manganese-catalyzed ozonation-influence of humic substances. *Water Res.* **1999**, 33, 785–793.
- (33) Ernst, M.; Lurot, F.; Schrotter, J. C. Catalytic ozonation of refractory organic model compounds in aqueous solution by aluminum oxide. *Appl. Catal., B.* **2000**, 47, 15–25.
- (34) Pecchi, G.; Reyes, P. Fe supported catalysts prepared by the sol-gel method. Characterization and evaluation in phenol abatement. *J. Sol.-Gel Sci. Technol.* **2003**, 26, 865–867.
- (35) Mulvaney, P.; Cooper, R.; Grieser, F.; Meisel, D. Charge trapping in the reductive dissolution of colloidal suspensions of Iron (III) oxides. *Langmuir* **1998**, 4, 1206–1211.
- (36) McKenzie, K. J.; Marken, F.; Hyde, M.; Compton, R. G. Nanoporous iron oxide membranes: Layer-by-layer deposition and electrochemical characterization of processes within nanopores. *New J. Chem.* **2002**, 26, 625–629.
- (37) Lake Lansing Watershed Advisory Committee. *Progress Report*; Ingham County Drain Commissioner's Office: Mason, Michigan, 1998.
- (38) Hoigné, J. *The Chemistry of Ozone in Water: Process Technologies for Water Treatment*; Plenum Publishing Corp.: New York, 1988.
- (39) *Standard Methods for Examination of Water and Wastewater*, 20th ed.; Clesceri, L. S., Greenberg, A. E., Eaton, A. D., Eds.; American Public Health Association: Washington, DC, 1998.
- (40) Munch, J. W.; Munch, D. J.; Winslow, S. D.; Wendelken, S. C.; Pepich, B. V. *Determination of carbonyl compounds in drinking water by pentafluorobenzyl hydroxylamine derivatization and capillary gas chromatography with electron capture detection*; Method 556.1; U.S. Environmental Protection Agency: Cincinnati, OH, 1998.
- (41) Chen, K. C. Ozonation, ultrafiltration, and biofiltration for the control of NOM and DBP in Drinking Water. Ph.D. Dissertation, Michigan State University, East Lansing, MI, 2003.

Received for review February 24, 2005. Revised manuscript received August 2, 2005. Accepted August 3, 2005.

ES0503938